Supporting information for

Boosting electrocatalysis activities of 2D ultrathin BiOX/rGO (X=F, Cl, Br, I) nanosheets as sulfur hosts: insight into the electronegativity effect of halogenated elements on the electrochemical performances of lithium-sulfur batteries

Meili Wang,[a,#] Yumiao Han,[b,#] Huaiqi Peng,[a] Ziqian Jin,[a] Hui Guan,[b] Shiyu Ma,[c,*] Xin Li,[a] Yunlai Ren,[a] Lixia Xie,[a] Xianfu Zheng,[a] Jianmin Zhang,[b,*] and Yutao Dong[a,d*]

[a] College of Science, Henan Agricultural University, Zhengzhou 450002, China

[b] College of Chemistry, Zhengzhou University, Zhengzhou 450001, China

[c] School of Chemical and Printing-Dyeing Engineering, Henan University of Engineering, Zhengzhou 450007, China

[d] Longzihu New Energy Laboratory, Zhengzhou Institute of Emerging Industrial Technology, Henan University, Zhengzhou 450000, China.

*Corresponding authors:

Yutao Dong, E-mail: ytdong@henau.edu.cn

Shiyu Ma, E-mail: msymsymsy@aliyun.com

Jianmin Zhang, E-mail: zhjm@zzu.edu.cn

# Meili Wang and Yumiao Han have contributed equally to this work.

Experimental Section

Materials

Natural graphite flakes with the average diameter of 200 meshes are purchased from Sigma-Aldrich Co. Ltd. (USA). Potassium permanganate (KMnO$_4$), hydrogen peroxide (H$_2$O$_2$), hydrochloric acid (HCl, 37%), and concentrated sulphuric acid (H$_2$SO$_4$, 98%) are received from Sinopharm Chemical Reagent Co. Ltd. (Shanghai, China). 1-methyl-2-pyrrolidinone (NMP) and glycol are received from Sinopharm Chemical Reagent Co. Ltd. (Shanghai, China). Bismuth nitrate pentahydrate (Bi(NO$_3$)$_3$.5H$_2$O), Sodium fluoride (NaF), Potassium bromide (KBr), Potassium chlorideand (KCl) and Potassium iodide (KI) are received from Shanghai Aladdin Biochenmical Technology Co. Ltd. Deionized water is used throughout. All the above chemicals are of analytical grade and are used as received.

Synthetic of BiOX/GO

The BiOX (X =F, Cl, Br, I) nanosheets are synthesized by solvothermal method. Graphene oxide (GO) is made by the Hummer's method. Graphene oxide (60 mg) is ultrasonically dispersed in a mixture of 30 mL water and 30 mL glycol to form a homogeneous solution. Subsequently, 2 mmol L^{-1} Bi(NO$_3$)$_3$5H$_2$O is added under vigorous stirring to obtain a uniform solution so that Bi^{3+} and GO are fully combined. Next, NaF is added to the above mixture under stirring for about 15 min. Finally, the mixture is transferred into a 100 mL Teflon-lined autoclave and maintained at 180 °C for 20 h to obtain black cylindrical hydrogel. Subsequently, the hydrogel is soak-ished in deionized water and freeze-dried. The synthesized samples with different concentrations of 0.2, 0.5, 1, 2, and 5 mmol L^{-1} Bi(NO$_3$)$_3$5H$_2$O and NaF are labeled as BiOF/rGO-0.2, BiOF/rGO-0.5, BiOF/rGO-1, BiOF/rGO-2, BiOF/rGO-5. If the concentration of materials mentioned in the article is not specified, all materials used

are BiOF/rGO-2.

The other BiOX (X= Cl, Br, I) nanosheets is prepared by the same procedure. Graphene oxide (60 mg) is ultrasonically dispersed in a mixture of 10 mL water and 50 mL glycol to form a homogeneous solution. Subsequently, 2 mmol L^{-1} $Bi(NO_3)_3 5H_2O$ is added under vigorous stirring to obtain a uniform solution so that Bi^{3+} and GO are fully combined. Next, KCl (KBr, KI) is added to the above mixture under stirring for about 15 min. Finally, the mixture is transferred into a 100 mL Teflon-lined autoclave and maintained at 150 °C for 12 h to obtain black cylindrical hydrogel. Subsequently, the hydrogel is soak-ished in deionized water and freeze-dried.

Synthesis of BiOX/GO-S

The BiOX/GO-S cathode is prepared by a simple melt-diffusion method. BiOX/GO powder and sulfur are evenly ground together (mass ratio 3:7), the mixture is heated to 155 °C in argon for 12 h, then heated to 200 °C for 1 h to remove excess sulfur on the surface, forming the BiOX/GO-S composite. The BiOX/GO-S, Super P and polyvinylidene (PVDF) are mixed according to the mass ratio of 7:2:1, and the 1-methyl-2-pyrrolidinone (NMP) as the solvent, stirring evenly to form the slurry. The slurry is evenly coated on the Al foil and dried in a vacuum oven at 50 °C for 12 h. Then it is cut into a circular electrode with a diameter of 14 mm.

Battery assembly and electrochemical performance testing

Li-S batteries are assembled using 2032-coin cells. The electrochemical performance is compared using BiOX/GO-S as the cathode and Li metal foil as the anode with PP (Gelgard2400) as a separator. The electrolyte is 1.0 M LiTFSI dissolved in DOL and DME (V/V=1:1) with 2 wt% $LiNO_3$. All battery assembly process is carried out in an argon-filled glove box (H_2O/O_2< 0.1 ppm). Constant-current charge/discharge tests are performed in the LAND CT2001A battery test system at room temperature for different

current densities (1 C = 1672 mA g^{-1}) with the voltage ranges of 1.7 V ~ 2.8 V. The cyclic voltammetry (CV) of the cells at 1.7 ~ 2.8 V and 0.1 mV s^{-1}, the lithium sulfide deposition and symmetrical cell tests are investigated using the CHI 660E electrochemical workstation. Electrochemical impedance (EIS) is recorded in the frequency range of $10^{\sim 2} \sim 10^5$ Hz.

Adsorption experiment and UV–vis measurements

Lithium polysulfide solution (Li$_2$S$_6$) is prepared by dissolving Li$_2$S and S (molar ratio 1:5) in a mixture of DOL:DME (v/v=1:1) and stirred at 60°C until brownish red liquid (0.2 M). The Li$_2$S$_6$ solution is diluted to 3 mM and 3 ml is taken as the adsorption solution, then add 10 mg of material as adsorbent (BiOF/rGO, BiOCl/rGO, BiOBr/rGO, BiOI/rGO) to the above solution and leave it for 12 h. After adding the adsorbent, digital photographs are taken periodically to observe the color change. After the adsorption reached equilibrium, the supernatant is taken and then diluted with DOL/DME (v/v=1:1) solvent for UV testing, and the residual material is dried in an argon-filled glove box for XPS characterization. (The whole adsorption process is done in a glove box filled with argon gas).

Li$_2$S precipitation experiments

Li$_2$S and S (molar ratio 1:7) are dissolved in the default electrolyte (1.0 M LiTFSI dissolved in DOL and DME (V/V=1:1) with 1 wt% LiNO$_3$) and stirred at 60 °C until complete dissolution to form a brownish red solution (0.2 M Li$_2$S$_8$). The BiOX/GO, polyvinylidene (PVDF) are mixed according to the mass ratio of 8:2, and the 1-methyl-2-pyrrolidinone (NMP) as the solvent, stirring evenly to form the slurry. The slurry is coated on Al foil and dried in a vacuum oven at 50 °C for 12 h, then it is cut into a circular with a diameter of 14 mm to serve as working electrodes, Li metal foil as the anode with PP (Gelgard 2400) as a separator. In a standard 2032-coin cell, 25 μL of

Li$_2$S$_8$ solution is added to the cathode and 25 μL of default electrolyte is added to the anode. Discharge at a constant current of 0.112 mA to 2.07 V consumes most of the higher-order polysulfide, followed by nucleation at a constant voltage of 2.05 V to grow Li$_2$S.

Symmetric cells

Lithium polysulfide solution (Li$_2$S$_6$) is prepared by dissolving Li$_2$S and S (molar ratio 1:5) in a mixture of the default electrolyte (1.0 M LiTFSI dissolved in DOL and DME (V/V=1:1) with 1 wt% LiNO$_3$) and stirred at 60°C until brownish red liquid (0.2 M). The BiOX/rGO, polyvinylidene (PVDF) are mixed according to the mass ratio of 8:2, and the 1-methyl-2-pyrrolidinone (NMP) as the solvent, stirring evenly to form the slurry. The slurry is coated on Al foil and dried in a vacuum oven at 50 °C for 12 h. Then it is cut into a circular with a diameter of 14mm to serve as working electrodes and counter electrode with PP (Gelgard 2400) as separator. In a standard 2032 coin-cell, 50 μl of Li$_2$S$_6$ solution is used as the electrolyte to assemble the cell. The CV evaluation of the symmetric cells is performed on an electrochemical workstation with a voltage of -1.0 V-1.0 V and a scan rate of 1 mV s^{-1}.

In-situ Raman spectroscopy and in-situ X-ray diffraction tests

The S@BiOF/rGO composites were mixed super P and PVDF binder in NMP solution (weight ratio is 7: 2: 1) to form a viscous slurry. Then the cathodes can be prepared after coating the slurry on porous aluminum mesh and drying for 12 h. The sulfur loading was around 1.0 mg cm^{-2}. In situ Raman spectroscopy analysis was performed using a two-electrode system (In situ Raman electrochemical cell, GAOSS UNION) with a quartz window. The Raman raster wavelength was 632 nm. In situ Raman spectra were collected in the spectral range of 100 to 600 cm^{-1} during charge and discharge at 0.2 C in the voltage range of 1.7 V to 2.8 V. Raman signals were acquired with a Raman

microscope (LabRAM HR Evolution, HORIBA).

In situ XRD measurements were performed using a two-electrode in-situ Li-S battery cell with a beryllium window. The cathode was prepared by coating a slurry of the active material onto the window and drying for 12 h. The sulfur loading was approximately 1.0 mg cm^{-2}. The cell was discharged and charged in the voltage range of 1.7-2.8 V at 0.2 C. In situ XRD spectra were collected using a Bruker D8 Advance diffractometer at a scanning rate of 0.6° min^{-1} within the 2θ range of 22–30°.

Material Characterization

Crystal structures are characterized with X-ray diffraction, using Cu-Kα radiation (Bruker D8 Advance). Scanning electron microscopy is performed with a JEOL JSM-6700F. Transmission electron microscopy (TEM) is conducted with a JEOL JEM-2010F. Surface chemistry is analyzed with X-ray photoelectron spectra on a thermal Fisher ESCALAB 250Xi spectrometer using a single Al Ka (1486 eV) light source. Thermogravimetric analysis is conducted with a STA 409 PC/PG at a heating rate of 10 °C min^{-1} under an Ar atmosphere. Raman spectra are acquired with a LabRAM HR Evolution and a 532 nm laser. UV-Vis spectroscopy is performed for lithium polysulfide adsorption experiments using a Perkin Elmer Lamda 25 UV/Vis spectrophotometer.
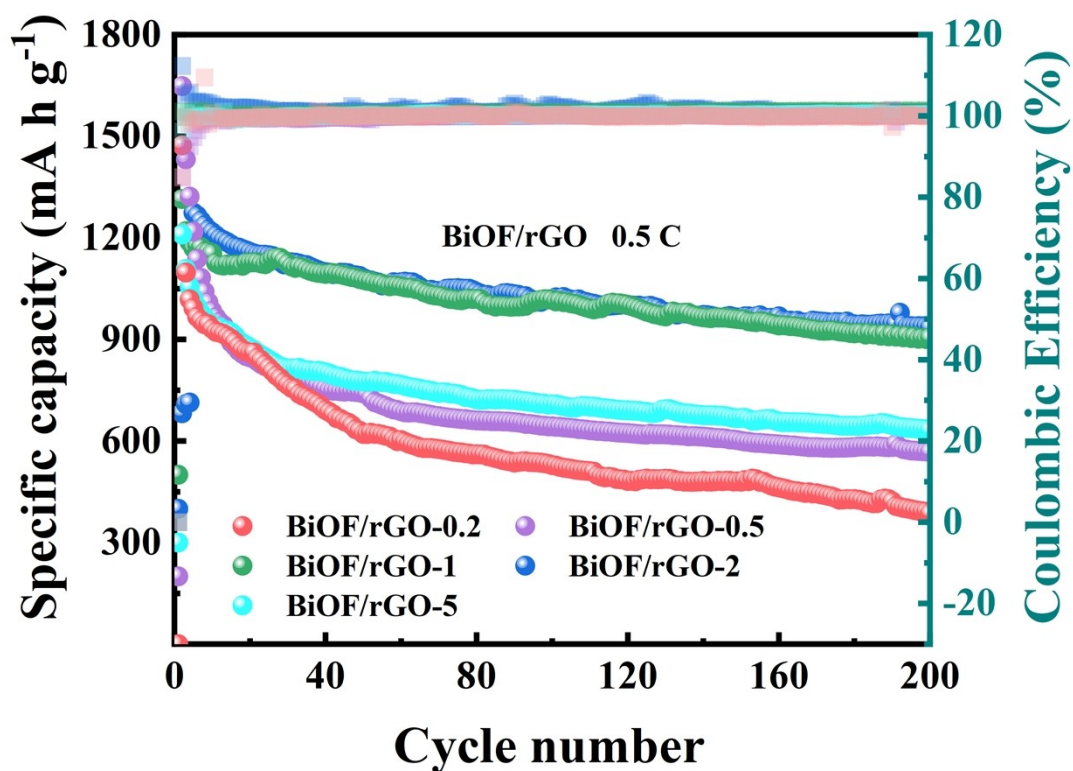
Fig. S1. Cycling performances of BiOF/rGO-S cathode at 0.5 C with different concentration of 0.2-5 mmol L^{-1} Bi(NO$_3$)$_3$·5H$_2$O and KX (X =F, Cl, Br, I).
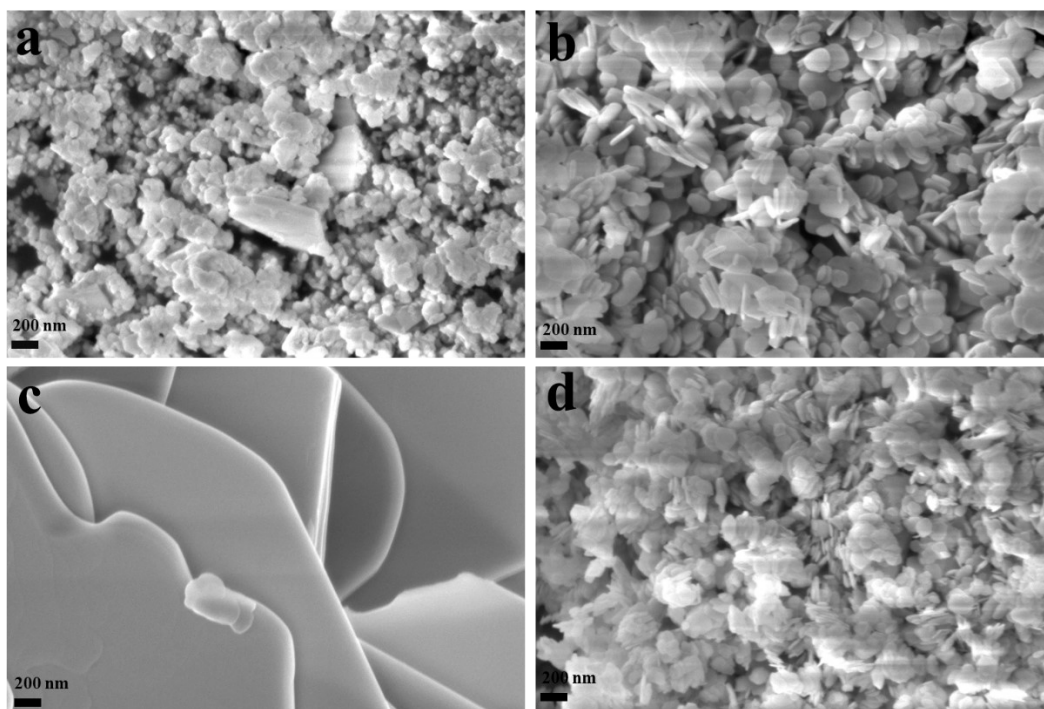
Fig. S2. SEM images of (a) BiOF (b) BiOCl (c) BiOBr (d) BiOI.
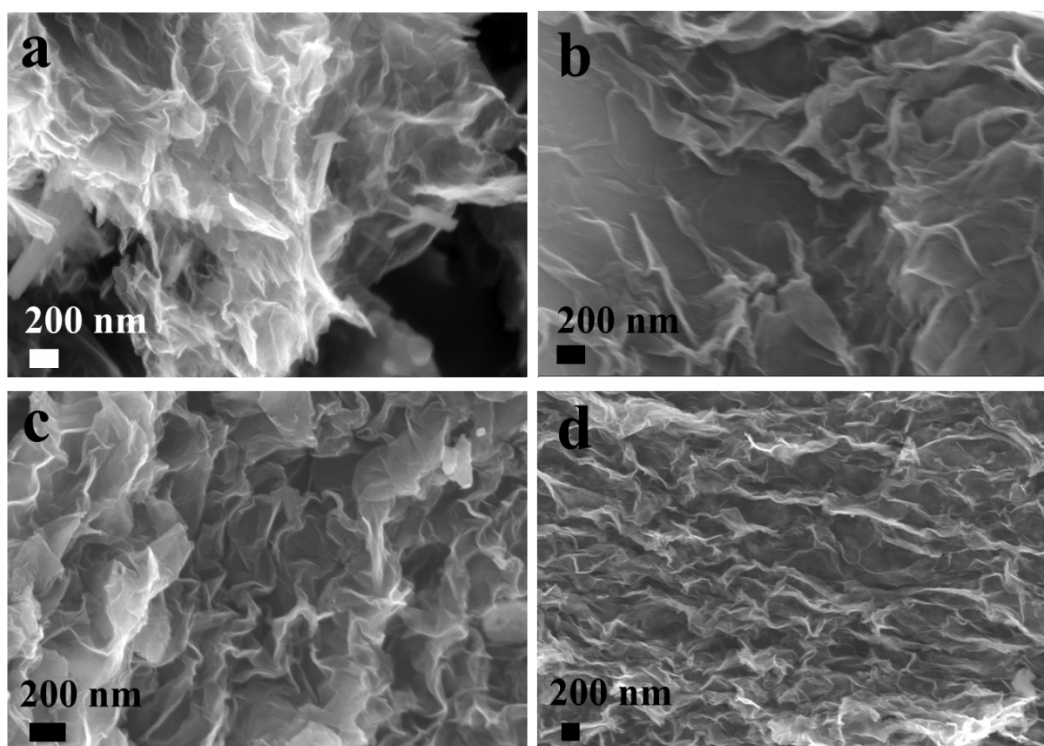

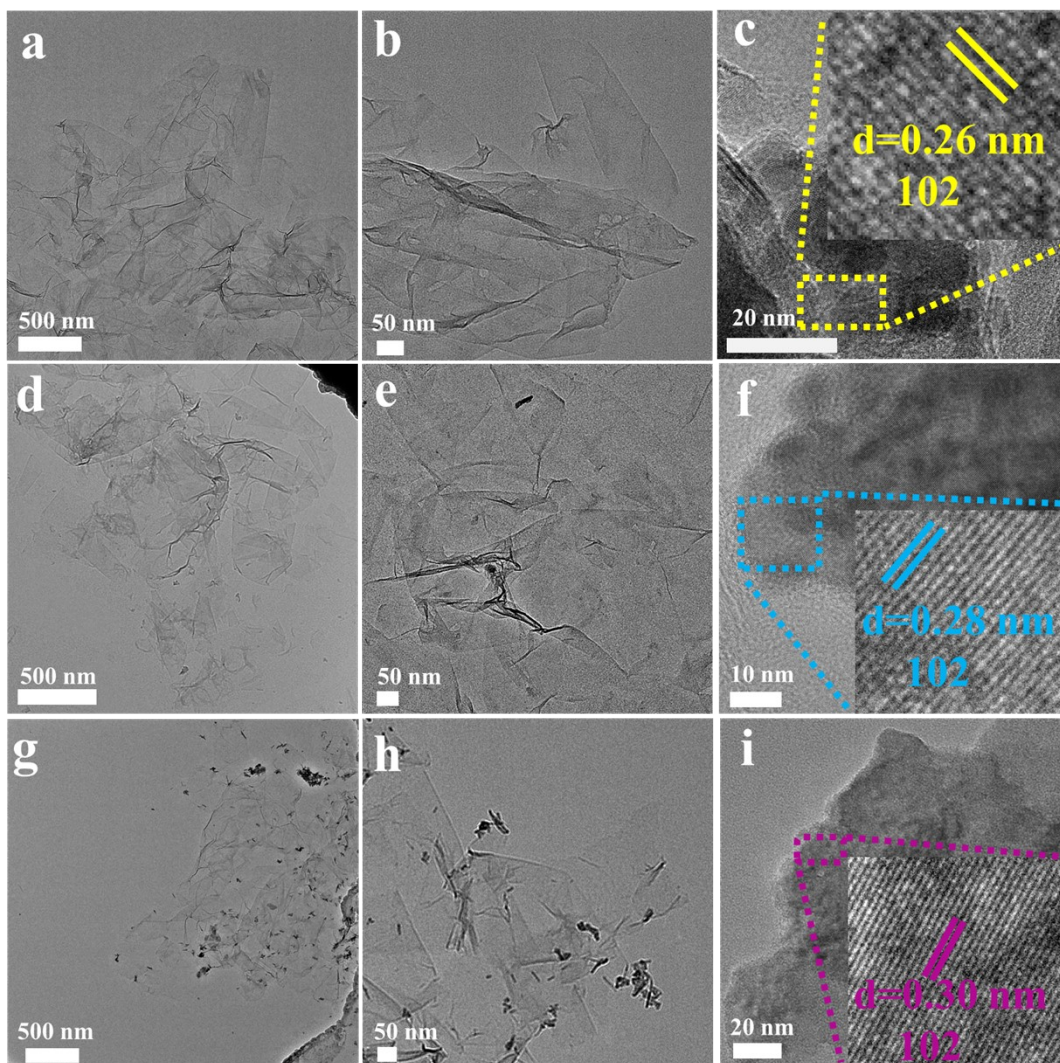**Fig. S3.** SEM images of (a) BiOF/rGO (b) BiOCl/rGO (c) BiOBr/rGO (d) BiOI/rGO.

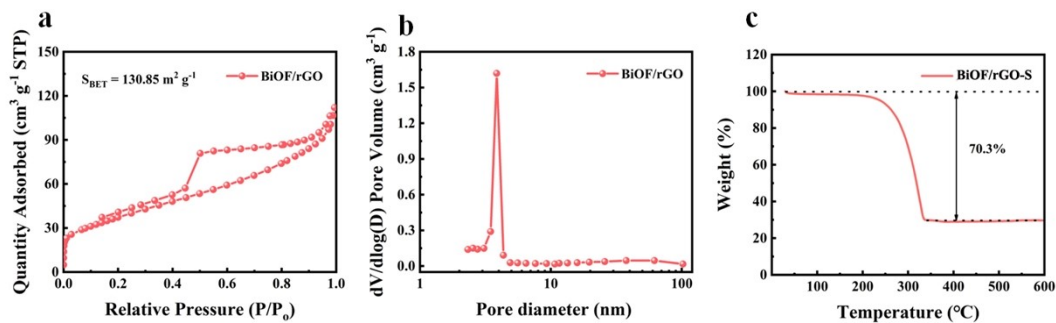**Fig. S4.** (a-c) TEM of BiOCl/rGO. (d-f) TEM of BiOBr/rGO. (g-i) TEM of BiOI/rGO.

Fig. S5. (a) Nitrogen adsorption−desorption isotherm, (b) the pore size distribution (inset) of BiOF/rGO, and (c) sulfur loading of BiOF/rGO-S.
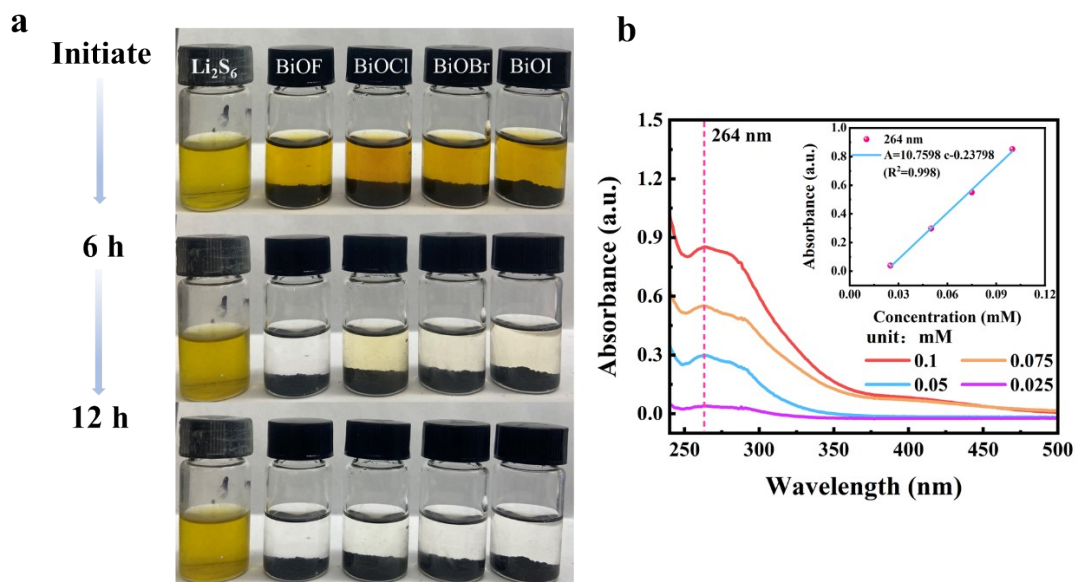

Fig. S6. (a) Visual adsorption experiment phenomena of BiOX/rGO in the Li_2S_6 solution. (b) UV-visible absorption spectra of blank solutions with different concentrations (the internal illustration shows the fitting curve between absorbance at 264 nm and Li_2S_6 concentration).
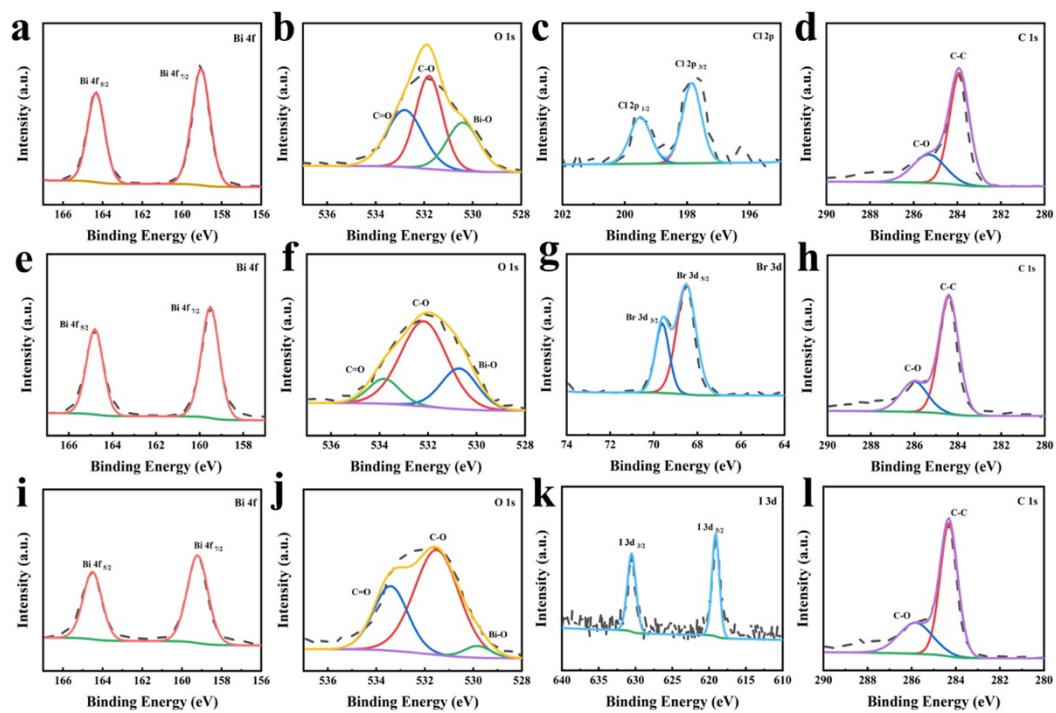
Fig. S7. (a-d) XPS spectra of Bi 4f, O 1s, Cl 2p, C 1s in BiOCl/rGO, respectively. (e-h) XPS spectra of Bi 4f, O 1s, Br 3d, C 1s in BiOBr/rGO, respectively. (i-l) XPS spectra of Bi 4f, O 1s, I 3d, C 1s in BiOI/rGO, respectively.

Table S1. The adsorption capacity of BiOF/rGO, BiOCl/rGO, BiOBr/rGO, BiOI/rGO.

	BiOF/rGO	BiOCl/rGO	BiOBr/rGO	BiOI/rGO
absorbance (a.u.)	0.05552	0.07748	0.12414	0.14862
concentration (mM)	0.027	0.029	0.034	0.036
adsorption capacity $(mg_{(Li2S6)}/mg_{(BiOX/rGO)})$	0.9187	0.9180	0.9165	0.9159

Table S2. The adsorption energy of BiOF/rGO, BiOCl/rGO, BiOBr/rGO and BiOI/rGO.

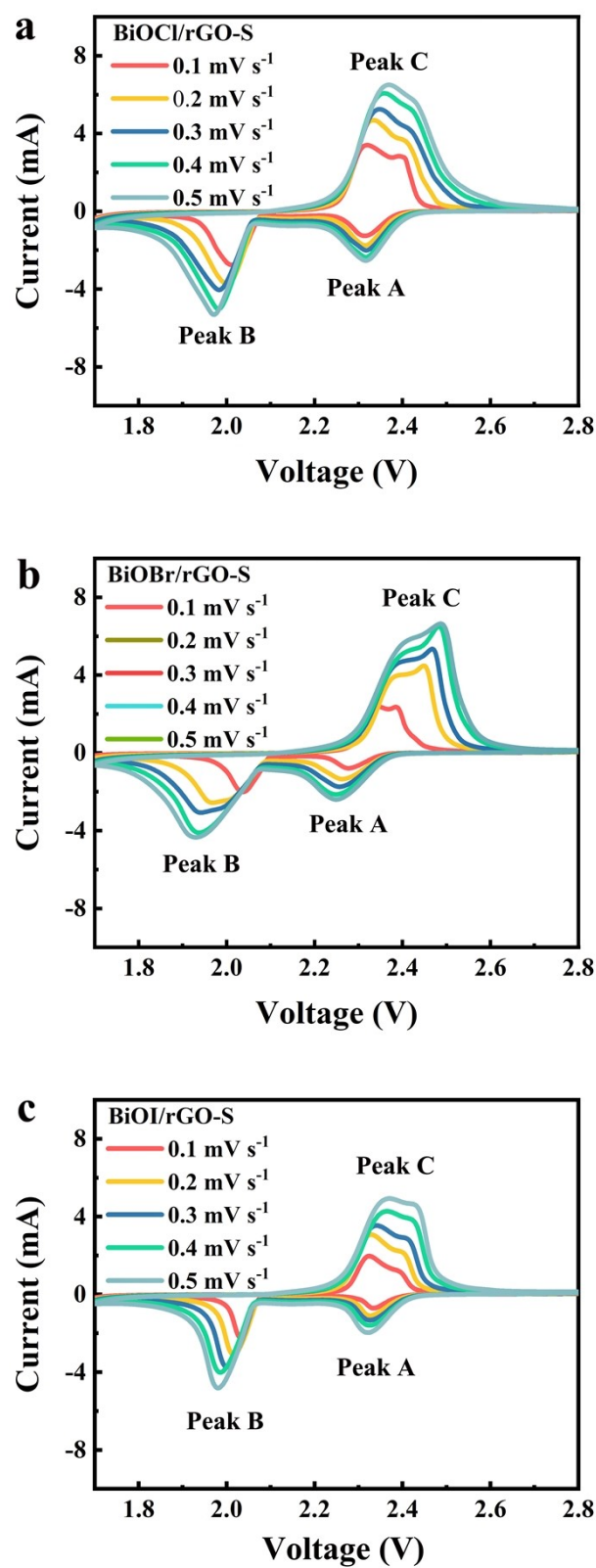| Energy of adsorption system		BiOF/rGO	BiOCl/rGO	BiOBr/rGO	BiOI/rGO
Li_2S_4	-617.89	2.34	0.95	0.77	0.74
Li_2S_6	-626.62	2.41	1.09	0.87	0.77
Li_2S_8	-635.33	2.96	1.11	1.22	1.15

Fig. S8. CV profiles of (a) BiOCl/rGO-S, (b) BiOBr/rGO-S and (c) BiOI/rGO-S cathodes at different scan rates.
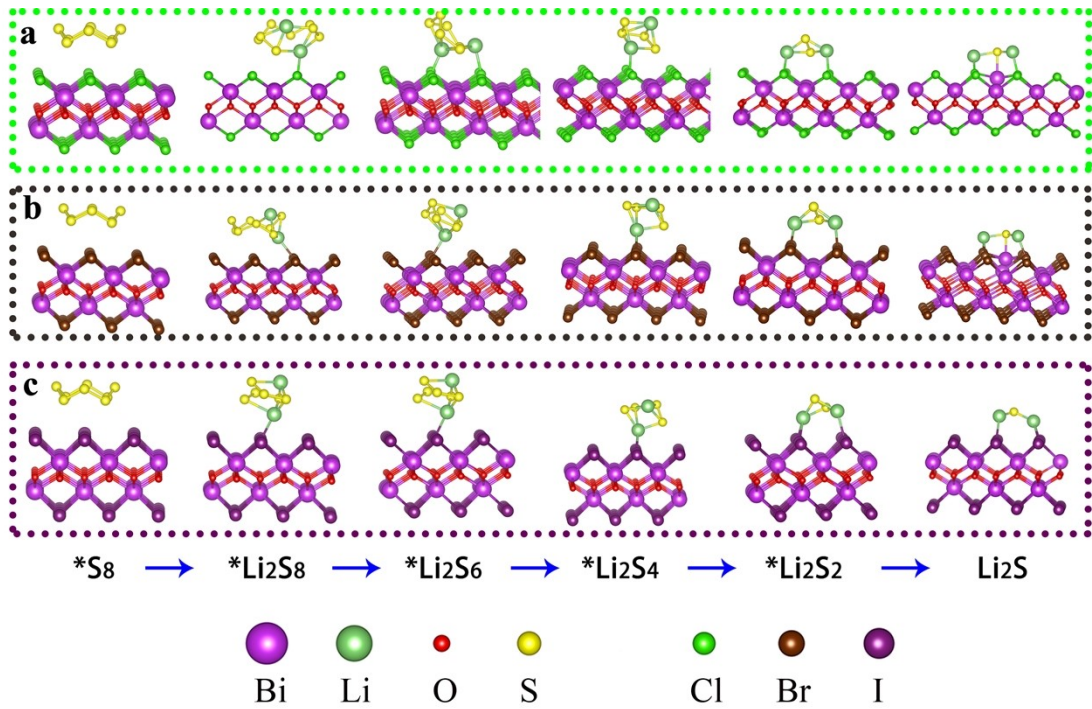
Fig. S9. Structural configurations of adsorbed LiPSs intermediates on the (a) BiOBr, (b) BiOCl, and (c) BiOI monolayers.
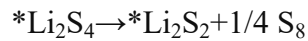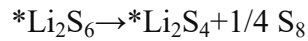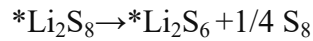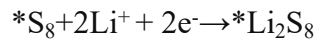
The density-functional theory (DFT) is employed in our first-principles calculations, utilizing the VASP code.[1-3] To describe the electronic-ion interaction, we employ the projector augmented wave method (PAW).[4] The energy cutoff of plane waves, which serve as the foundation for the wave function, is set at 450 eV. The electron exchange-correlation function is treated using a generalized gradient approximation (GGA) in the form proposed by Perdew, Burke, and Ernzerhof (PBE) .[5] The conjugate gradient (CG) algorithm is employed to optimize both atomic positions and lattice vectors, showcasing its prowess in achieving optimal configurations. The convergence precision for energy and force is meticulously set at 10^{-5} eV and 0.1 eV/Å respectively, ensuring utmost accuracy in the calculations. To eliminate any interference from neighboring images, a vacuum region larger than 10 Å is thoughtfully incorporated into the

simulation setup. In order to accurately sample the Brillouin zone (BZ) integration, a meticulous grid of 3×3 k-points is utilized for computations. Furthermore, the inclusion of van der Waals interaction through the employment of Grimme's DFT-D3 method further enhances the fidelity of our results.[6] The free energy change for the electrochemical steps of sulfur reduction reaction (SRR) is determined using methodologies established in prior research.[7]

In the simulations of polysulfide adsorption on the BiOX monolayer, a 3×3 supercell is employed to model the BiOX monolayer. Overall, during the discharging process of Li-S batteries, an S_8 molecule undergoes a remarkable 16-electron transformation accompanied by the formation of eight Li_2S molecules.

$S_8+16Li^++16e^-\rightarrow 8Li_2S$
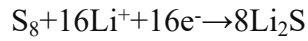
The elementary steps of generating one Li_2S molecule are described as follows,

$*S_8+2Li^+ + 2e^-\rightarrow *Li_2S_8$

$*Li_2S_8\rightarrow *Li_2S_6 +1/4\ S_8$

$*Li_2S_6\rightarrow *Li_2S_4+1/4\ S_8$

$*Li_2S_4\rightarrow *Li_2S_2+1/4\ S_8$

$*Li_2S_2\rightarrow *Li_2S+1/8\ S_8$

where * stands for an active site on the catalytic surface.

For each step of SRR, the reaction Gibbs free energy is given by

$$\Delta G = \Delta E + \Delta E_{ZPE} - T\Delta S \tag{1}$$

The free energy as computed by DFT (ΔG), is accompanied by contributions from energy difference between products and reactants (ΔE), zero-point energy (ΔE_{ZPE}) and entropy (ΔS).

The free energy change for the SRR electrochemical steps can be obtained from the following expressions:

ΔG_1

$$= \left(E_{* Li_2S_8} + E_{ZPE(* Li_2S_8)} - TS_{* Li_2S_8}\right) - \left(E_{* S_8} + E_{ZPE(* S_8)} - TS_{* S_8}\right) - 2(E_{Li} + E_{ZPE(Li)} - T$$

$$(2)$$

ΔG_2

$$= \left(E_{* Li_2S_6} + E_{ZPE(* Li_2S_6)} - TS_{* Li_2S_6}\right) + \frac{1}{4}\left(E_{* S_8} + E_{ZPE(* S_8)} - TS_{* S_8}\right) - (E_{* Li_2S_8} + E_{ZPE(*}$$
$$- TS_{* Li_2S_8})$$

$$(3)$$

ΔG_3

$$= \left(E_{* Li_2S_4} + E_{ZPE(* Li_2S_4)} - TS_{* Li_2S_4}\right) + \frac{1}{4}\left(E_{* S_8} + E_{ZPE(* S_8)} - TS_{* S_8}\right) - (E_{* Li_2S_6} + E_{ZPE(*}$$
$$- TS_{* Li_2S_6})$$

$$(4)$$

ΔG_4

$$= \left(E_{* Li_2S_2} + E_{ZPE(* Li_2S_2)} - TS_{* Li_2S_2}\right) + \frac{1}{4}\left(E_{* S_8} + E_{ZPE(* S_8)} - TS_{* S_8}\right) - (E_{* Li_2S_4} + E_{ZPE(*}$$
$$- TS_{* Li_2S_4})$$

$$(5)$$

ΔG_5

$$= \left(E_{* Li_2S} + E_{ZPE(* Li_2S)} - TS_{* Li_2S}\right) + \frac{1}{8}\left(E_{* S_8} + E_{ZPE(* S_8)} - TS_{* S_8}\right) - (E_{* Li_2S_2} + E_{ZPE(* Li_2}$$
$$TS_{* Li_2S_2})$$

$$(6)$$

Table S3. Binding energies of S_8/polysulfides adsorbed on BiOF, BiOCl, BiOBr, and BiOI monolayers in electrolyte solvent molecules (DME and DOL).

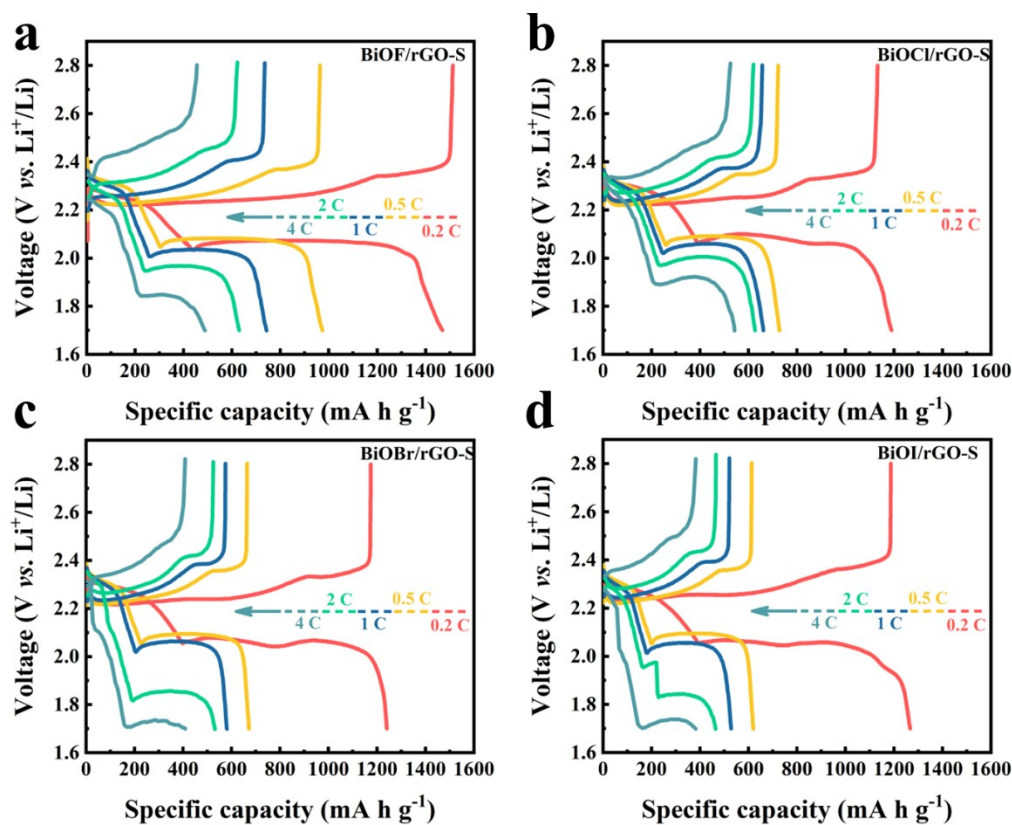| Absorption energy (eV)	BiOF	BiOCl	BiOBr	BiOI
S_8	1.76	0.84	0.79	0.81
Li_2S_8	2.96	1.11	1.15	1.22
Li_2S_6	2.41	1.09	0.77	0.87
Li_2S_4	2.34	0.95	0.74	0.77
Li_2S_2	3.11	1.38	1.08	1.18
Li_2S	4.15	2.11	1.15	1.89

Fig. S10. Charge/discharge curves of four electrodes at different rates (a) BiOF/rGO-S (b) BiOCl/rGO-S (c) BiOBr/rGO-S (d) BiOI/rGO-S.
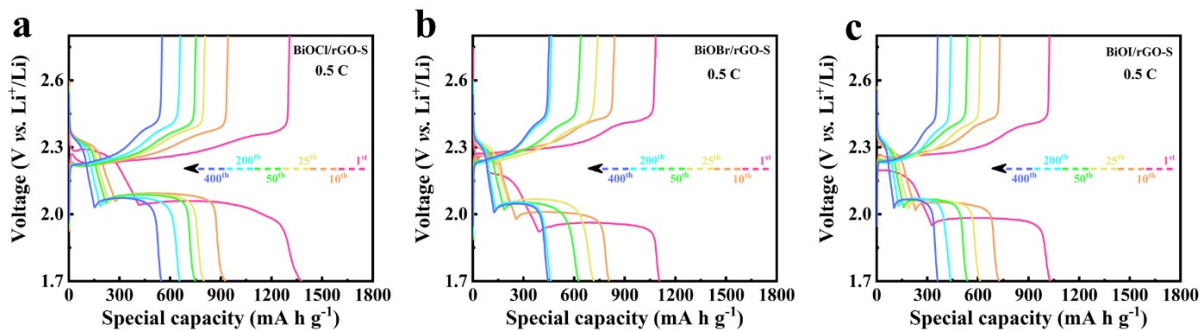
Fig. S11. Charge/discharge curves of the three electrodes at 0.5 C (a) BiOCl/rGO-S (b) BiOBr/rGO-S and (c) BiOI/rGO-S.

References

1. G. Kresse and J. Hafner, Ab initiomolecular dynamics for liquid metals, *Phys. Rev. B*, 1993, **47**, 558-561.

2. G. Kresse and J. Hafner, Ab initiomolecular dynamics for open-shell transition metals, *Phys. Rev. B*, 1993, **48**, 13115-13118.

3. G. Kresse and J. Furthmiiller, Efficiency of ab-initio total energy calculations for metals and semiconductors using a plane-wave basis set. , *Comput. Mater. Sci*, 1996, **6**, 15-50.

4. P. E. Blochl, Projector augmented-wave method, *Phys. Rev. B*, 1994, **50**, 17953-17979.

5. J. P. Perdew, K. Burke and M. Ernzerhof, Generalized Gradient Approximation Made Simple, *Phys. Rev. Lett.*, 1996, **77**, 3865-3868.

6. S. Grimme, J. Antony, S. Ehrlich and H. Krieg, A consistent and accurate ab initio parametrization of density functional dispersion correction (DFT-D) for the 94 elements H-Pu, *J. Chem. Phys.*, 2010, **132**, 154104.

7. M. A. Al-Tahan, Y. Dong, A. E. Shrshr, X. Kang, H. Guan, Y. Han, Z. Cheng, W. Chen and J. Zhang, Modulating of MoSe$_2$ functional plane via doping-defect engineering strategy for the development of conductive and electrocatalytic mediators in Li-S batteries, *J. Energy Chem.*, 2022, **75**, 512-523.